

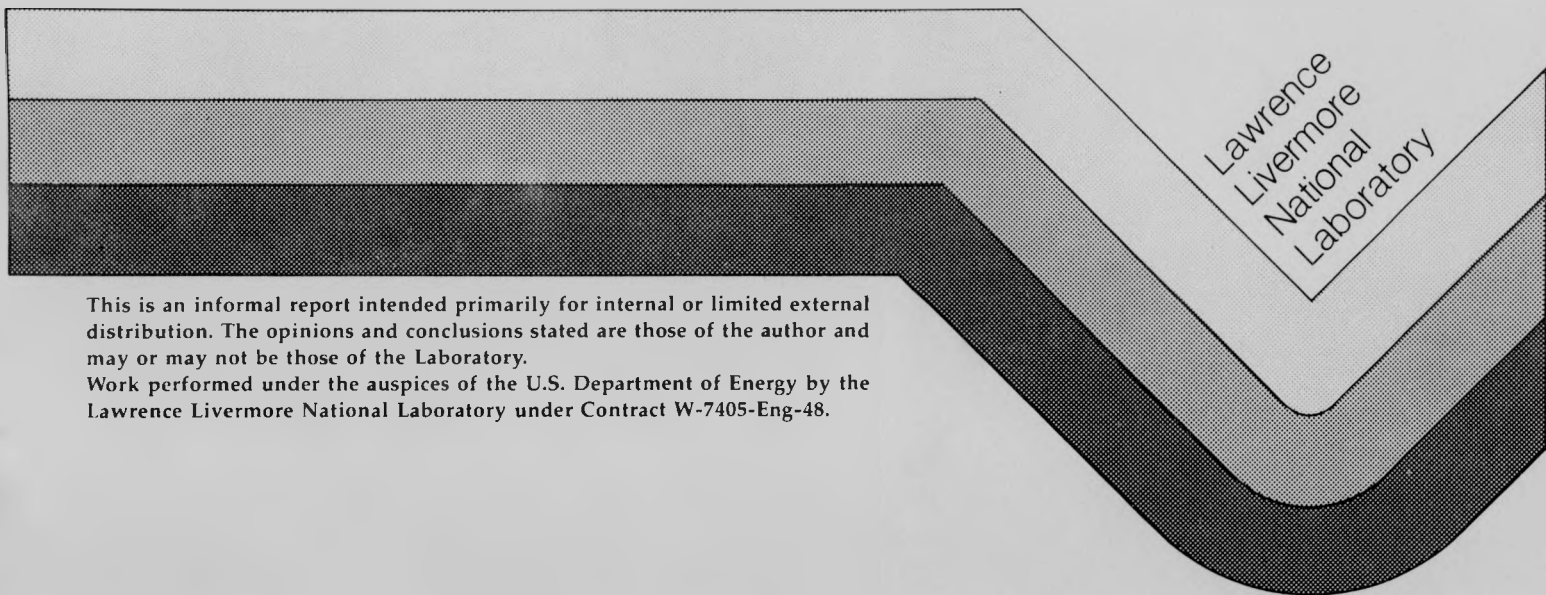
10
5-21-90 yss (1)

UCID- 16986-89-2/3/4

**OIL SHALE QUARTERLY REPORT
APRIL-DECEMBER 1989**

R. Cena

April 16, 1990



This is an informal report intended primarily for internal or limited external distribution. The opinions and conclusions stated are those of the author and may or may not be those of the Laboratory.
Work performed under the auspices of the U.S. Department of Energy by the Lawrence Livermore National Laboratory under Contract W-7405-Eng-48.

DISCLAIMER

This report was prepared as an account of work sponsored by an agency of the United States Government. Neither the United States Government nor any agency thereof, nor any of their employees, makes any warranty, express or implied, or assumes any legal liability or responsibility for the accuracy, completeness, or usefulness of any information, apparatus, product, or process disclosed, or represents that its use would not infringe privately owned rights. Reference herein to any specific commercial product, process, or service by trade name, trademark, manufacturer, or otherwise does not necessarily constitute or imply its endorsement, recommendation, or favoring by the United States Government or any agency thereof. The views and opinions of authors expressed herein do not necessarily state or reflect those of the United States Government or any agency thereof.

DISCLAIMER

Portions of this document may be illegible in electronic image products. Images are produced from the best available original document.

DISCLAIMER

This document was prepared as an account of work sponsored by an agency of the United States Government. Neither the United States Government nor the University of California nor any of their employees, makes any warranty, express or implied, or assumes any legal liability or responsibility for the accuracy, completeness, or usefulness of any information, apparatus, product, or process disclosed, or represents that its use would not infringe privately owned rights. Reference herein to any specific commercial products, process, or service by trade name, trademark, manufacturer, or otherwise, does not necessarily constitute or imply its endorsement, recommendation, or favoring by the United States Government or the University of California. The views and opinions of authors expressed herein do not necessarily state or reflect those of the United States Government or the University of California, and shall not be used for advertising or product endorsement purposes.

This report has been reproduced
directly from the best available copy.

Available to DOE and DOE contractors from the
Office of Scientific and Technical Information
P.O. Box 62, Oak Ridge, TN 37831
Prices available from (615) 576-8401, FTS 626-8401.

Available to the public from the
National Technical Information Service
U.S. Department of Commerce
5285 Port Royal Rd.,
Springfield, VA 22161

<u>Price Code</u>	<u>Page Range</u>
A01	Microfiche
<u>Papercopy Prices</u>	
A02	1- 10
A03	11- 50
A04	51- 75
A05	76-100
A06	101-125
A07	126-150
A08	151-175
A09	176-200
A10	201-225
A11	226-250
A12	251-275
A13	276-300
A14	301-325
A15	326-350
A16	351-375
A17	376-400
A18	401-425
A19	426-450
A20	451-475
A21	476-500
A22	501-525
A23	526-550
A24	551-575
A25	576-600
A99	601 & UP

CONTENTS

List of Tables.....	iii
List of Illustrations.....	iii
1. Initial Coke Formation on the Burnt Shale Present in a Solid-Recycle Fluidized-Bed Retort.....	1
2. Coking of Flash-Pyrolyzed Shale-Oil Vapors in a Downstream Packed-Bed Reactor.....	7
2.1 Introduction.....	7
2.2 Experimental.....	7
2.3 Results.....	9
2.4 Conclusions and Discussion.....	10
2.5 References.....	11
3. Laboratory Pilot-Plant Development.....	12
3.1 Air-Lift Pipe.....	12
3.2 Delayed-Fall Combustor.....	16
3.3 Fluid-Bed Classifier.....	16
4. Short-Term Carbonate Decomposition in Green River Oil Shale.....	22
4.1 Abstract.....	22
4.2 Introduction.....	22
4.3 Experimental.....	23
4.4 Results.....	23
4.5 Discussion and Conclusions.....	25
4.6 References.....	28

LIST OF TABLES

Table 1-1. Fischer Assay yields are achieved at higher recycle ratios when burn temperature increases.....	3
Table 1-2. Variables tested for their influence on yield from a solid-recycle retort.....	5
Table 2-1. Characteristics of oxidized-shale coker bed.....	7
Table 2-2. Carbon and hydrogen balance (experiment cok3, 500 °C pyrolysis, 600 °C coker temperature).....	10
Table 3-1. Typical lift-pipe test results (pressure data).....	16
Table 3-2. Delayed-fall combustor test results.....	16
Table 3-3. Results of particle-size segregation tests.....	19

LIST OF ILLUSTRATIONS

Fig. 1-1. Fluidized-bed pyrolysis with burnt shale present (>95% carbon balance), Anvil Points 24 gal./ton shale (AP24) and New Albany 13 gal./ton shale (NA13).....	1
Fig. 1-2. Unburnt retorted shale does not promote yield loss.....	2
Fig. 1-3. Chemistry can be used to improve yields when NA13 (-20/+35 mesh) is pyrolyzed at 475 °C.....	3
Fig. 1-4. Steam also enhances the yield from AP24 at all recycle ratios.....	4

MASTER

LIST OF ILLUSTRATIONS—(Continued)

Fig. 2-1. Apparatus used for flash pyrolysis of shale with subsequent exposure of the pyrolysis products to oxidized shale. Raw shale is dropped into a sand-fluidized bed at 500 °C. Oil vapors and gas are passed through a packed bed of oxidized shale. Oil vapors and gas leaving the packed bed are mixed with oxygen and burnt in a combustor. The concentration of CO₂ and H₂O in the burnt gas are measured every second by a mass spectrometer. The amount of carbon and hydrogen left in the coker and left on the retorted shale in the fluidized bed can be determined by using the rotary valve to direct the flow of oxygen in to the coker (B) and then to the fluidized bed (C).....8

Fig. 2-2. Shale was pyrolyzed at 500 °C in a fluidized bed, and the oil and gas produced were passed over oxidized shale at 600 °C. The first CO₂ and H₂O peak represents the amount of oil and gas that passed over the oxidized shale and did not coke. The area of the second peak would represent the amount of coke formed on the oxidized shale except that some of the CO₂ reacts with the oxidized shale bed to form carbonates. The same problem occurs when the char on the retorted shale is burnt. Char yield was found to be approximately 18% of the raw shale organic carbon, based on measurements without the oxidized shale bed. The coke yield is determined by difference.....9

Fig. 3-1. Solid heat carrier.12

Fig. 3-2. Hot-recycled-solid (HRS) process.....13

Fig. 3-3. Lift-pipe test apparatus.....14

Fig. 3-4. Typical lift-pipe test results (trapping data).15

Fig. 3-5. Delayed-fall combustor test model.17

Fig. 3-6. Fluidized-bed classifier model.....18

Fig. 3-7. Details of the gas distributor plate.19

Fig. 3-8. Fluidized-bed mixer model.....20

Fig. 3-9. Packed-bed pyrolyzer.....21

Fig. 4-1. Carbon dioxide evolution from retorted Green River shale heated at 700 °C in a laboratory fluidized bed, experiment cd7. Fluidizing gas was argon. The CO₂ concentration is proportional to the rate of carbonate decomposition. Carbon monoxide is assumed to be formed by the char reduction of CO₂.23

Fig. 4-2. Repeat of the experiment shown in Figure 1 with a slightly larger sample size and faster argon flow rate, experiment cd8.....24

Fig. 4-3. Extent of carbonate decomposition during the first few minutes of heating of Green River oil shale at 700 °C. From integration of the data of Figs. 1 and 2.25

Fig. 4-4. Extent of carbonate decomposition in Green River shale as a function of time at 700 °C calculated from the model of Camp and Braun.....25

Fig. 4-5. Comparison of experimental values of short-term carbonate decomposition to calculated values.26

Fig. 4-6. Percent thermal carbonate decomposition at 750 °C calculated from the Camp and Braun model, showing the fraction of char required. Based on a retorted shale containing 45% carbonates (mostly dolomite) and 2.5 wt% char.27

1. INITIAL COKE FORMATION ON THE BURNT SHALE PRESENT IN A SOLID-RECYCLE FLUIDIZED-BED RETORT

Conversion of kerogen to char and gas results in reduced oil yields. Recently, we have been investigating coke formation on solid in a fluidized-bed pyrolyzer. For convenience, we differentiate chars of three types:

Type A: Coke that forms directly from the kerogen as it pyrolyzes and generates volatile products.

Type B: Coke that forms as volatile reactive intermediates or metastable oil precursors contact surface sites on retorted and burnt shale.

Type C: Coke that is deposited as stable hydrocarbon products are further pyrolyzed.

This last category can be subdivided into thermal and catalytic coking/cracking processes. This section focuses on efforts to understand initial formation of char type B; we use a laboratory fluidized bed for our experiments. See Sec. 2 for discussion of type C coking.

The claim that char formation in the immediate vicinity of evolving volatiles (type B) differs from later char formation (type C) rests on the observation that relatively small quantities of burnt shale in a laboratory fluidized bed result in greater-than-expected charring. Figure 1-1 shows the volatile hydrocarbon yield (expressed in % of organic carbon evolved as oil + gas) as the amount of burnt shale in the fluid bed varied from 0 to ~6 times the amount of raw shale added. We noted a 5–10% decrease in yield with only 0.5 g of burnt shale in 100 g of sand (burnt/raw ratio = 1).

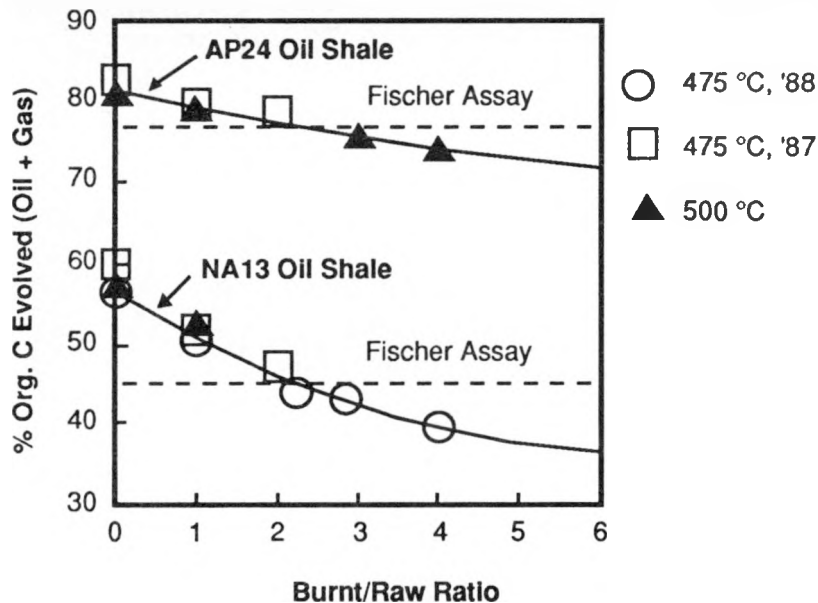


Fig. 1-1. Fluidized-bed pyrolysis with burnt shale present (>95% carbon balance), Anvil Points 24 gal./ton shale (AP24) and New Albany 13 gal./ton shale (NA13).

Hot-recycled-solid (HRS) retorting processes recycle burnt oil shale as the solid heat carrier. However, as noted, burnt shale is not inert, and it promotes conversion of volatile hydrocarbons to coke. We have developed a fluidized-bed pyrolyzer and a novel detector that allow us to study coke make and obtain accurate carbon balances from bench-scale flash pyrolysis and combustion experiments. The apparatus gives us a very sensitive tool to study the effect of changes in

experimental conditions on the volatile hydrocarbon yield. It provides an opportunity to search for ways to moderate the undesirable properties of burnt shale present in a fluidized-bed pyrolyzer.

We find that volatile organic carbon release is inversely related to the quantity of burnt shale in the fluidized sand bed (see Fig. 1-1). Eastern oil shale (a 13-gal./ton New Albany shale, called NA13) is relatively more susceptible than is western oil shale (a 24-gal./ton Green River oil shale from Anvil Points Mine, AP24) to yield losses from oxidized shale. Although NA13 suffers relatively greater volatile losses in the presence of burnt shale than does AP24, absolute losses are essentially equivalent for the two since AP24 yields more volatiles than does NA13. In a clean sand bed, NA13 gave $130 \pm 10\%$ of the assay yield on flash pyrolysis; hydrocarbon production dropped below $90 \pm 5\%$ of assay when the burnt/raw ratio in the fluidized-bed pyrolyzer was 4 (all yields include gas). AP24 yielded $115 \pm 5\%$ of assay with no burnt shale present, 95% of assay at a burnt/raw ratio = 4. These results are in excellent agreement with our own pilot plant experience [1-1, 1-2], with studies of Carter and co-workers using NA13 [1-3], and with the 1956 report by DiRicco and Barrick on laboratory pyrolysis of a Mahogany Zone Green River oil shale [1-4].

For our initial experiments, we used Devonian oil shale (NA13). We wanted to vary pyrolysis and burn conditions significantly while minimizing changes in surface area (and reactivity) that accompany carbonate mineral decomposition (i.e., in the western shale case). Remarkable improvements in yields could be achieved by altering the properties of solid present. Perhaps our most important observation was the following: Retorted but unburned Devonian shale is like sand; no yield loss is noted even at high recycle ratios. Figure 1-2 compares yield versus recycle ratio results when retorted (but not burned) Devonian oil shale was present with those when burnt shale was present.

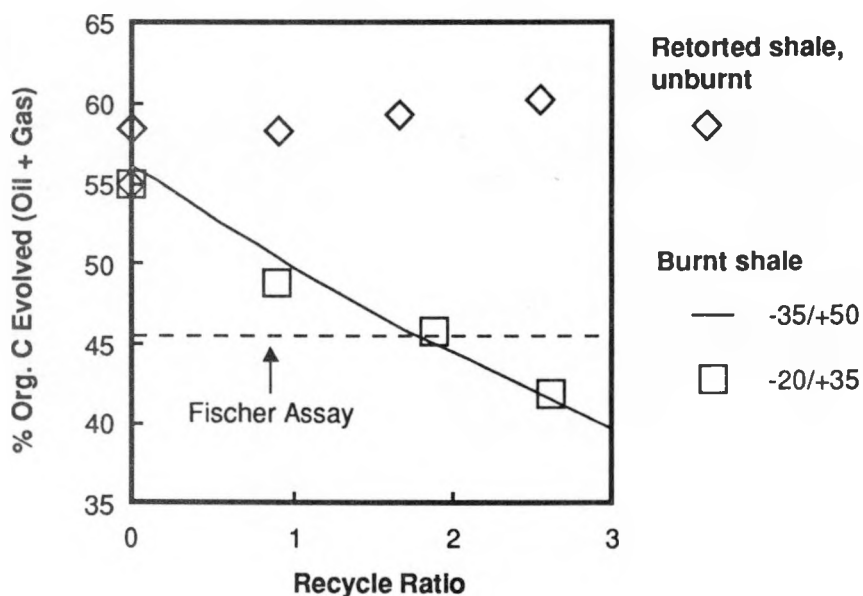


Fig. 1-2. Unburnt retorted shale does not promote yield loss.

Furthermore, raising the burn temperature of the spent shale proved beneficial. This observation also has important processing implications. Table 1-1 shows that oil-plus-gas yields that are greater than Fischer assay (FA) are realized with recycle ratios as high as 5 when the combustor is run hot (i.e., above 700°C). It might be noted that 700°C is just above the decomposition temperature of iron sulfate, which has been shown to be a particularly detrimental additive under batch pyrolysis conditions [1-5]. There was no indication that the solid fused. For the Colorado oil shale (AP24), a slightly higher burn temperature proved desirable. At burn

temperatures above 600 °C, however, extensive dolomite decomposition occurred and the increased shale surface area enhanced coking activity.

Table 1-1. Fischer Assay yields are achieved at higher recycle ratios when burn temperature increases.

Combustor Temp. (°C)	Recycle Ratio with FA Yield*
480	2.0
725	3.6
785	5.1

*For NA13, FA yield is 45.5% organic carbon evolved as oil-plus-gas.

The yield of hydrocarbons was also very sensitive to chemical modifications of the solid (e.g., burnt shale) in the bed. Some yield improvement compared to burnt shale (but not compared to sand) was often possible. For example, steam (50% in argon) or ammonia (3% in argon) decreased coke formation but did not totally negate the impact of burnt Devonian shale (Fig. 1-3). Steam has a long history of use as a coking inhibitor in hydrocarbon crackers. Furthermore, iron compounds in the shale mineral matter can react with steam to add to the hydrogen donor pool. For example:

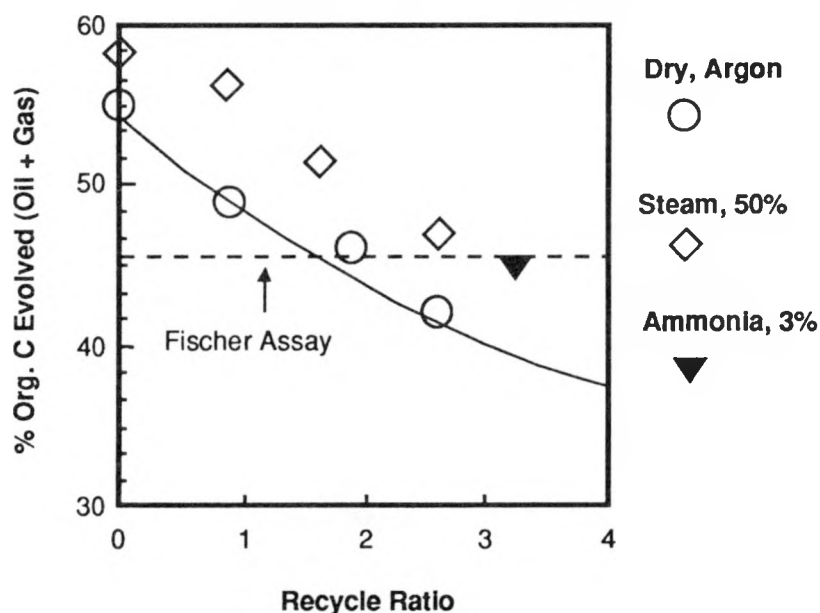
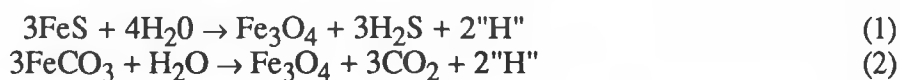


Fig. 1-3. Chemistry can be used to improve yields when NA13 (-20/+35 mesh) is pyrolyzed at 475 °C.

Western oil shale kerogen releases (at best) 85% of its carbon as oil-plus-gas, but 95% of its hydrogen. Devonian kerogen is even more hydrogen deficient, so a small increase in H-donors ("H") has a dramatic effect on hydrocarbon yield.

Steam promotes carbonate mineral decomposition, and we have yet to obtain a satisfactory separation of the organic and inorganic carbon evolved from steam retorting of western oil shale. We did carry out steam- and ammonia-swept experiments on a carbonate-free western oil shale obtained by acid leaching the raw shale. Yield improvements were similar to those seen in our eastern oil shale experiments (see Figs. 1-3 and 1-4). While acid leaching removes iron from a raw shale (and AP24 has only about half the iron content of NA13), this is balanced by the Colorado kerogen's lesser demand for hydrogen. Furthermore, a very slight yield improvement under dry pyrolysis conditions was apparently obtained simply by removing the carbonate minerals. However, these results remain in question since it was difficult to know the recycle ratio accurately when working with acid-leached AP24. In the presence of steam, the material rapidly disintegrated to dust and was blown from the bed.

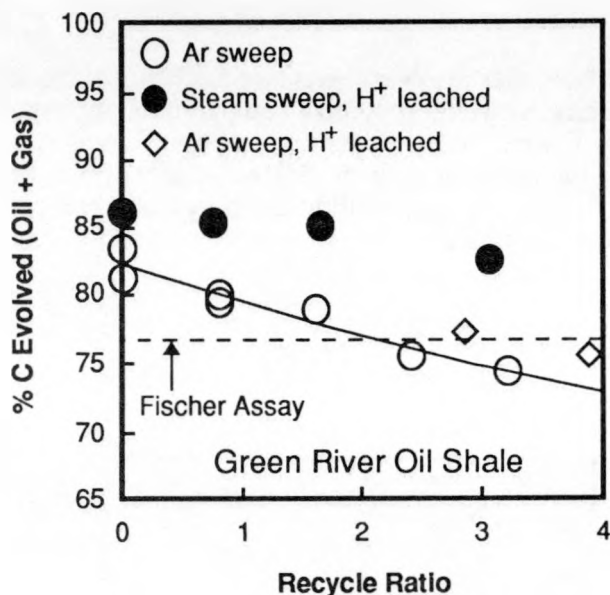


Fig. 1-4. Steam also enhances the yield from AP24 at all recycle ratios.

We added NH_3 to the fluidizing gas in an attempt to demonstrate the acidity of those active surface sites where coking took place. However, the impact of ammonia was so similar to that of steam (see Fig. 1-3) that both may function primarily as H-donors. Iron compounds are well-known catalysts for NH_3 synthesis. Under our ambient pressure conditions ammonia should undergo rapid iron-catalyzed decomposition to N_2 and H_2 (or H-donors). When both ammonia and steam were present in the fluidizing gas, the yield from western shale was equal to that with steam alone. Steam inhibits iron-catalyzed ammonia decomposition.

Factors tested for their impact on yield are summarized in Table 1-2. With shale and recycle ratio the same, variation of pyrolysis temperature (475 or 500 °C) or particle size (-20/+35 or -35/+50 mesh) had no detectable influence on yield. These minor variations may have produced yield losses or gains that were below our detection limit of $\pm 2\%$ relative. At pyrolysis temperatures below 450 °C, incomplete pyrolysis and/or incomplete volatilization resulted in low hydrocarbon yields, perhaps, because of coking of type A.

Table 1-2. Variables tested for their influence on yield from a solid-recycle retort.

<u>Variable</u>	<u>Impact*</u>
Nature of Sweep Gas	
a) Steam	+
b) NH ₃	+
c) Propane	0
System Effects	
a) Dust in effluent filter	0
b) Pyrolyzer temperature	0
Recycled-Shale Properties	
a) Quantity	-
b) Particle size	0
c) Surface area and roughness	-
d) Burn temperature	+
e) Retorted (not burnt)	+
Feed Oil Shale Properties	
a) Particle size	0
b) Source	0
c) Air exposure	0
d) Acid leaching (NA13 only)	0

* 0 = $\pm 2\%$ effect; + = $>2\%$ positive effect; - = $>2\%$ negative effect

Our findings have direct implications for the design and construction of a pilot or commercial scale solid-recycle retort that will produce the maximum oil yield. For example, yield loss should be moderated by reducing the burnt shale's oxidizing properties. To accomplish this, a reducing gas stream (pyrolysis gas or products from char gasification) might be introduced to the surge tank at the combustor outlet or to the burnt shale/raw shale mixer. The introduction of steam, particularly in the latter stages of pyrolysis, should be given a carefully evaluation. Steam should increase hydrocarbon generation at the price of additional dust. Finally, the combustor temperature should be high, if relatively inactive burnt shale is to be generated.

Unfortunately, we have limited opportunities to test successfully many of the above suggestions in the laboratory. It is particularly difficult to duplicate the short-time, high-temperature burn conditions of a large-scale process. Especially in our work with Green River oil shale, we must burn at low temperatures or otherwise avoid excessive carbonate decomposition. However, some answers can be obtained through inverse chromatography studies and experiments with burnt shale positioned downstream from the kerogen undergoing pyrolysis (see Sec. 2). These should tell us if it is transient, highly reactive oil precursors or highly active solid that account for the very rapid initial rate of coking.

References

- 1-1. R. J. Cena and R. G. Mallon, "Results and Interpretation of Rapid-Pyrolysis Experiments Using the LLNL Solid-Recycle Oil Shale Retort," in *Proceedings of the 19th Oil Shale Symposium* (Colorado School of Mines Press, Golden, 1986), p. 102.
- 1-2. R. J. Cena and R. W. Taylor, "Results of Rapid Pyrolysis Experiments Using Eastern U.S. Oil Shale in the Livermore Solid-Recycle Retort," in *Proceedings of the Eastern Oil Shale Symposium* (Univ. of Kentucky Press, Lexington, 1986), p. 31.

- 1-3. S. D. Carter, "Fluidized Bed Pyrolysis Kinetics of New Albany Oil Shale," in *Proceedings of the Eastern Oil Shale Symposium* (Univ. of Kentucky Press, Lexington, 1986), p. 45.
- 1-4. L. DiRicco and P. L. Barrick, "Pyrolysis of Oil Shale," *Ind. Eng. Chem.* **48**, 1316 (1956).
- 1-5. A. E. Lewis, T. T. Coburn, R. J. Cena, and D. W. Camp, "LLNL Oil Shale Project Review," in *Proceedings of the Second Annual Oil Shale Contractors Meeting*, T. C. Bartke, Ed. (DOE/METC-86/6045, Morgantown, 1986), p. 78.

2. COKING OF FLASH-PYROLYZED SHALE-OIL VAPORS IN A DOWNSTREAM PACKED-BED REACTOR

2.1 Introduction

Currently, the only practical way of obtaining oil from oil shale is heat. However, hot oil vapors are not stable; they tend to change (crack) into lighter oils and gases with time. Oil vapors also react on hot surfaces to form a carbon-rich solid (coke) and lighter gases. The higher the temperature the more rapid are these oil-loss reactions, particularly cracking. Coke-forming reactions depend on the nature of the solid surface and the surface area to oil vapor ratio.

These facts impact the design and operation of oil-shale retorts. Optimum yield is achieved with rapid shale heating and rapid removal and cooling of the oil vapors to ensure minimum contact with high-surface-area materials.

A 10% increase in oil and gas yield relative to FA for Green River shale has been confirmed in laboratory flash-pyrolysis experiments by means of an inert solid followed by rapid cooling of oil vapors [2-1]. Other shales show higher gains in yield (relative to FA) with flash pyrolysis [2-2]. However, pilot-scale retorting utilizing flash pyrolysis by means of hot oxidized shale followed by rapid quenching of the oil vapors has not resulted in oil-yield gains over FA [2-3, 2-4, 2-5].

The goal of the present work is to determine the extent and rate of coke formation by the action of oxidized shale on flash-generated oil in a downstream packed-bed coker. This corresponds to type C coking (see Sec. 1 for definition).

2.2 Experimental

The shale used was AP24C, a sample of oil shale from the Green River formation at the Anvil Points Mine in Colorado, having a grain size range between 0.4 and 0.6 mm. The shale sample contained 9.81 wt% organic carbon and a total hydrogen content of 1.24 wt%. Oxidized shale was prepared by first retorting the shale under FA conditions, then burning the shale at 600 °C in an argon-20% oxygen mixture. The combustion temperature was chosen to be in the low end of the range as used in the hot-recycle-solid (HRS) pilot retort at Lawrence Livermore National Laboratory (LLNL) to minimize carbonate decomposition.

The flash-pyrolysis/coking apparatus is shown in Fig. 2-1. It is constructed of stainless steel. Raw shale (0.56 g) is dropped into a 500 °C fluidized bed. The fluidized bed is 90 g of quartz sand between 0.4 and 0.6 mm in diameter. Fluidization is with preheated argon flowing at approximately 4 liters/minute.

Oil vapors and gas from retorting shale pass to the packed-bed coker. In the present experiments the coker was at either 500 °C or 600 °C. The packed-bed coker is a "U" tube containing oxidized shale. The tube is 27 cm long with an inside diameter of 1.1 cm. The tube volume is 24.4 cm³. The packed bed of oxidized shale is described in Table 2-1.

Table 2-1. Characteristics of oxidized-shale coker bed.

Mass of Bed	18.8 g
Volume of bed	18 cm ³
Particle Size	1.5–2.2 mm
Particle Volume	5×10 ⁻⁴ cm ³ /particle
Particle Density	2.5 g/cm ³
Particles in bed	14,000
External Surface Area	2×10 ⁻³ m ² /g
Internal Surface Area	3 m ² /g

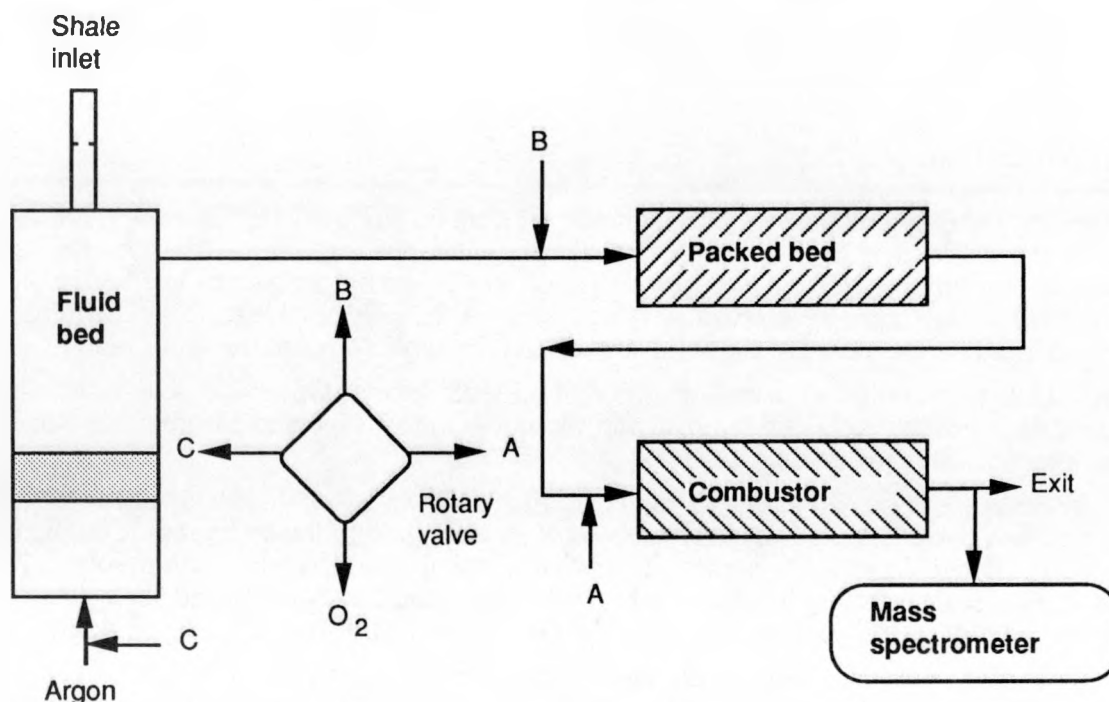


Fig. 2-1. Apparatus used for flash pyrolysis of shale with subsequent exposure of the pyrolysis products to oxidized shale. Raw shale is dropped into a sand-fluidized bed at 500 °C. Oil vapors and gas are passed through a packed bed of oxidized shale. Oil vapors and gas leaving the packed bed are mixed with oxygen and burned in a combustor. The concentration of CO₂ and H₂O in the burnt gas are measured every second by a mass spectrometer. The amount of carbon and hydrogen left in the coker and left on the retorted shale in the fluidized bed can be determined by using the rotary valve to direct the flow of oxygen in to the coker (B) and then to the fluidized bed (C).

Oil vapors which pass through the coker in the argon stream are mixed with pure oxygen to bring the mixture to 19% oxygen. The mixture is passed into a combustor. This contains platinum heated to 1000 °C in a silica-glass tube. The concentration of CO₂ and H₂O from the combustion of uncoked oil vapors is measured every second by means of an on-line mass spectrometer. The amount of oil and gas produced is calculated from these concentration measurements and the gas flow rate.

The exposure time of the oxidized shale in oil vapors was equal to the retorting time, ~2 minutes at 500 °C. The concentration of oil vapors at the entrance of the coker was a maximum of ~0.1 vol%—based on the measured initial concentration of CO₂ (3%) and an oil molecular weight of 300.

The amount of hydrogen in coke was determined by diverting the oxygen from the combustion tube to the coking unit inlet by means of the rotary valve and measuring the concentration of H₂O as a function of time. Likewise, the hydrogen in the char in the retorted shale remaining in the fluidized bed was measured by flowing oxygen through the fluidized bed.

We planned to make a direct measurement of the amount of coke formed by measuring the amount of CO₂ produced when oxygen was diverted from the combustion tube to the inlet of the coking unit by means of the rotary valve. We found the amount of CO₂ released during coke combustion at 600 °C was about 25% less than the amount of oxygen consumed. Carbon dioxide appears to be reacting with CaO and other components of the oxidized shale to form carbonates. In principle, we can calculate the amounts of coke and char by measuring the amount of oxygen

consumed rather than the amount of CO_2 released. This calculation is subject to error because of volume of oxygen-free gas resulting from the switching of the oxygen from the combustor to the coker and from the coker to the fluidized bed.

Coke is therefore determined by difference. It is the difference between the total amount of raw-shale organic carbon and the amount of char, oil, and gas. Char is the organic carbon remaining in the fluidized bed; it is about 18% of the raw-shale organic carbon, based on measurements without an oxidized-shale bed downstream.

In one experiment, the amount of raw shale utilized was reduced from 0.56 g to 0.27 g to find if a higher ratio of oxidized shale to oil would increase the fraction of oil converted to coke.

In four sequential experiments, the oxidized shale in the coker was not burned between drops of raw shale. This was to find out if covering the oxidized shale surfaces with coke decreased the tendency to form coke and, if so, the amount of coke necessary to cause the decrease.

2.3 Results

Figure 2-2 gives concentrations of CO_2 and H_2O as a function of time for an experiment called cok3. In this experiment, the temperature of pyrolysis was 500°C and the temperature of the oxidized shale was 600°C .

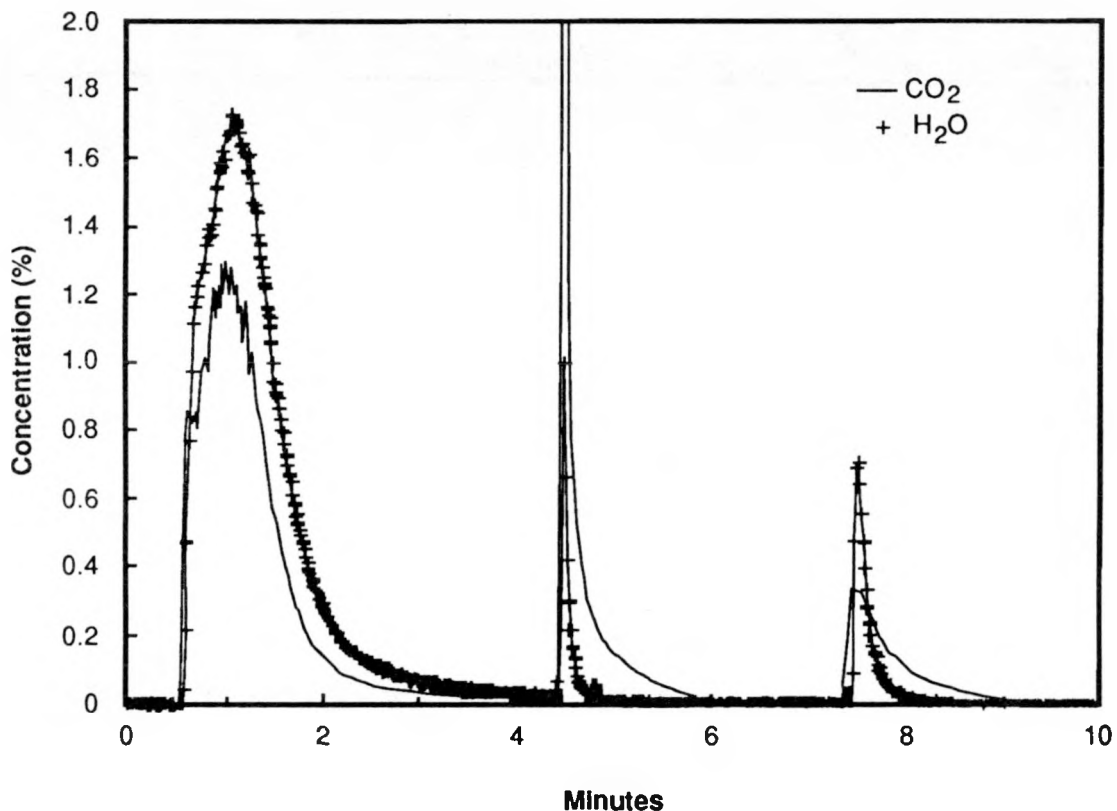


Fig. 2-2. Shale was pyrolyzed at 500°C in a fluidized bed, and the oil and gas produced were passed over oxidized shale at 600°C . The first CO_2 and H_2O peak represents the amount of oil and gas that passed over the oxidized shale and did not coke. The area of the second peak would represent the amount of coke formed on the oxidized shale except that some of the CO_2 reacts with the oxidized-shale bed to form carbonates. The same problem occurs when the char on the retorted shale is burned. Char yield was found to be approximately 18% of the raw-shale organic carbon, based on measurements without the oxidized shale bed. The coke yield is determined by difference.

The area of the first CO₂ and H₂O peak corresponds to the amount of carbon and hydrogen in oil vapor and hydrocarbon gas released by flash pyrolysis and not coked. The area of the other peaks corresponds to the amounts of coke and char. As already discussed, the area of the second and third CO₂ peaks are less than the amount of oxygen consumed because of the capture of CO₂ to form carbonates in the oxidized-shale bed in the coker.

Table 2-2 gives the results for experiment cok3.

Table 2-2. Carbon and hydrogen balance (experiment cok3, 500 °C pyrolysis, 600 °C coker temperature).

	C		H		H/C ratio
	mmole	%	mmole	%	
Oil & gas	2.0	44	6.3	87	3.1
Coke	1.75	38*	0.48	6.6	0.3
Char	0.82	18**	0.48	6.6	0.6
Totals	4.57	100	7.26	100	1.6
Raw Shale	4.57		6.94		1.5
Balance			5% gain		

Coke Yield = 1.1×10^{-3} (g carbon in coke/g oxidized shale)

*By difference

**Assumed

When the coker temperature was reduced from 600 °C to 500 °C, the amount of coke formed did not decrease but remained the same.

Does coke on oxidized shale reduce additional coke formation? In the set of four sequential experiments directed to this question, we found that the oil and gas yield of the first three drops of the oxidized shale was the same as when freshly-oxidized shale was present in the coker. However, the oil and gas yield at the fourth drop increased 30%; the coke yield decreased accordingly. Thus, after the coke accumulation reached approximately 3 mg/g of oxidized shale, the rate of additional coke formation decreased sharply.

The presence of oxidized shale, or of oxidized shale coated with coke, resulted in a broader CO₂ peak during the combustion of the oil and gas (compared to the peak when oxidized shale was absent).

2.4 Conclusions and Discussion

During the 80-millisecond transit time of oil vapor through the coker, nearly half of the carbon forms coke on oxidized shale. This shows that shale-oil vapors have a strong tendency to coke on oxidized shale and that coke-forming reactions can be very fast at 600 °C.

The action of oxidized shale, whether coated with coke or not, appears to be much like the packing on a chromatographic column. Adsorption and desorption of oil take place, adding time for coke to form.

In these experiments, the mass of oxidized shale was 34–70 times the mass of the raw shale that was heated to release oil. In processing terms, this is a very high recycle ratio. (In LLNL's HRS pilot plant, the amount of oxidized shale present during retorting was approximately 4 times the mass of shale retorted, a recycle ratio of 4.)

The fraction of raw-shale organic carbon converted to coke in the present experiments was 36%. This fraction remained constant at coker temperatures of 500 °C and 600 °C and when the mass of oxidized shale was 34 or 70 times the mass of raw shale pyrolyzed. Singleton and Mallon [2-6] found that the same fraction of organic carbon in raw shale converted to coke when exposure of oil vapors on coke-coated oxidized shale was longer than 10 seconds at 600 °C. This evidence strongly suggests that 36% represents an effective maximum fraction of the carbon that can be converted to coke for this Green River shale.

We can estimate the thickness of coke necessary for repression of additional coking. When the coke deposit was more than approximately 3 mg coke/g of oxidized shale, coke formation slowed. Amorphous carbon has a bulk density of 1.8 g/cm³, suggesting that coke formation will be slowed when the coke volume is more than $\sim 1.7 \times 10^{-3}$ cm³/g oxidized. The surface area of oxidized Green River shale is approximately 3 m²/g, according to measurements by Slettevold et al. [2-7]. Thus, if the coke layer has uniform thickness and the density of amorphous carbon, the critical depth of the layer is 6×10^{-10} m. The amount of graphite adsorbed as a monolayer on the same surface area would amount to 2.3 mg/g of oxidized shale. (Graphite has an area of 5.1×10^{-20} m²/ring; a ring has on the average 6 carbon atoms, each shared by three adjacent rings.) It appears that a monolayer of coke is sufficient to sharply decrease the coking tendency of oxidized shale.

The implications to processing are significant. The rate of coke formation during the deposition of a monolayer of coke is very rapid. The amount of the loss of oil to form a monolayer of coke is proportional to the recycle ratio. In the case of Green River shale retorted at a recycle ratio of 4, the loss will be 8 mg/g raw shale. The amount of organic carbon converted to oil by flash pyrolysis in the absence of oxidized shale is approximately 70 mg/g of raw shale. Thus, the loss to a monolayer of coke will be approximately 10% of the oil. A reduction of the recycle ratio to 2 could reduce this loss to 5%.

2.5 References

- 2-1. E. R. Bissell, A. K. Burnham, and R. L. Braun, "Shale Oil Cracking and Diagnostics," *I&EC Process Des. Dev.* **24**, 381 (1985).
- 2-2. T. T. Coburn, R. W. Taylor, and C. J. Morris, "Laboratory Studies of New Albany Shale Flash Pyrolysis Under Solid-Recycle Conditions: Chemistry and Kinetics," in *Proceedings of the Eastern Oil Shale Symposium* (Univ. of Kentucky Press, Lexington, 1988), p. 325.
- 2-3. R. J. Cena and R. G. Mallon, "Results and Interpretation of Rapid-Pyrolysis Experiments Using the LLNL Solid-Recycle Oil Shale Retort," in *Proceedings of the 19th Oil Shale Symposium* (Colorado School of Mines Press, Golden, 1986), p. 102.
- 2-4. R. J. Cena and R. W. Taylor, "Results of Rapid Pyrolysis Experiments Using Eastern U.S. Oil Shale in the Livermore Solid-Recycle Retort," in *Proceedings of the Eastern Oil Shale Symposium* (Univ. of Kentucky Press, Lexington, 1986), p. 31.
- 2-5. N. V. Dung, G. C. Wall, and G. Kastl, "Continuous Fluidized Bed Retorting of Condor and Stuart Oil Shales in a 150mm Diameter Reactor," *Fuel* **66**, 372 (1987).
- 2-6. M. F. Singleton and R. G. Mallon, private communication (1990).
- 2-7. C. A. Slettevold, A. H. Biermann, and A. K. Burnham, *A Surface-Area and Pore-Volume Study of Retorted Oil Shale*, Lawrence Livermore National Laboratory, Livermore, Calif., UCRL-52619 (1978).

3. LABORATORY PILOT-PLANT DEVELOPMENT

The pilot plant currently under construction uses the HRS system. Figure 3-1 shows diagrammatically the use of solid heat carrier as the source of heat for shale pyrolysis. Retorted shale is burned in a combustor to increase the shale temperature. A portion of the burned shale is then returned to the retort and mixed with raw shale. The width of the flow bands on the diagram indicate the relative mass flow rates in the system. As indicated, the rate at which burned shale enters the retort is much greater than the rate at which burned shale exits the system.

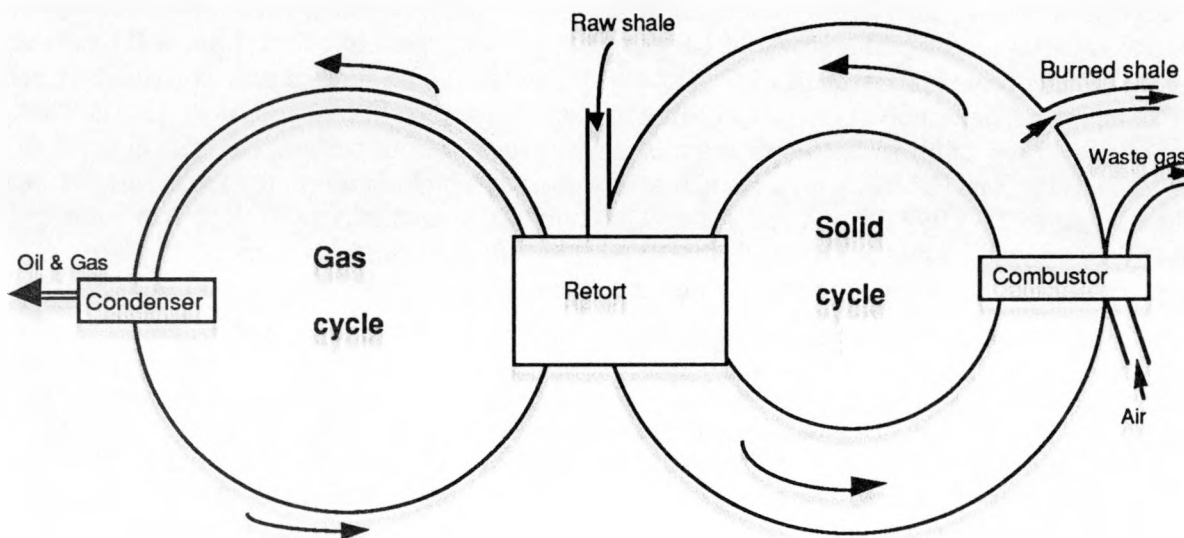


Fig. 3-1. Solid heat carrier.

Figure 3-2 shows the major components in the solid circulation loop. Starting at the bottom of the figure, these are:

- Air-lift pipe
- Delayed-fall combustor
- Fluidized-bed classifier
- Fluidized-bed mixer
- Packed-bed pyrolyzer

To aid in the design of these components, we have performed tests at ambient temperature and pressure using plastic models. These tests will be described in the order listed above.

3.1 Air-Lift Pipe

The lift pipe serves two functions. First, it transports retorted shale from the pyrolyzer to the top of the tower. Second, it provides part of the char combustion. The lift-pipe test was performed in the apparatus shown in Fig. 3-3. The lift pipe consists of two sections of different diameter. The bottom portion of the lift, for a height of about 1 meter, has an inside diameter of 3.8 cm. It is in this portion that particles are accelerated by the lifting air. Above the acceleration region, the pipe inside diameter is 6.0 cm. The small diameter of the lower portion provides high air velocity and reliable solid pickup and acceleration. The larger diameter in the upper portion of the pipe results in somewhat lower velocity of air and solid. This lower velocity provides longer residence time in the lift and increases the amount of combustion that will occur in the lift pipe and be used in the pilot plant. In the test model, the two pipes that are joined at the bottom of the

apparatus were made of lucite. It is at this point that pickup of the solid by the air occurs. The transparent tubing made possible direct observation of the pickup process.

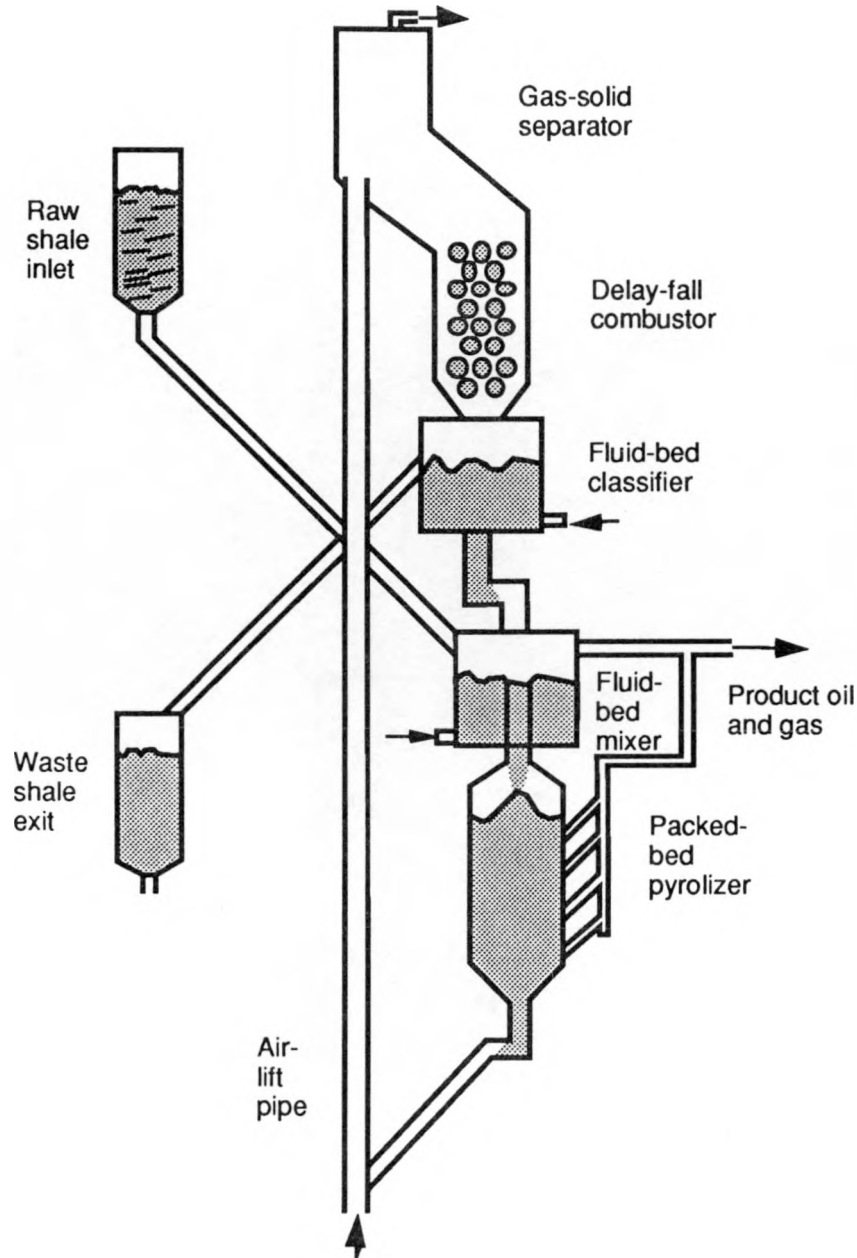


Fig. 3-2. Hot-recycled-solid (HRS) process.

The lift-pipe model was equipped with two remote-operated fast-acting gate valves. One of these was at the point at which the pipe diameter changes near the bottom of the lift. The other valve was a short distance below the air-solid separator near the top of the lift. Vertical separation of the valves was 8 m. By means of simultaneous closing of these valves with the lift in operation, the solids in the lift between the valves were trapped as a means of measuring particle residence time. This trapped material was then removed, weighed, and its particle size analyzed to determine the speed with which particles of various sizes move upward in the pipe.

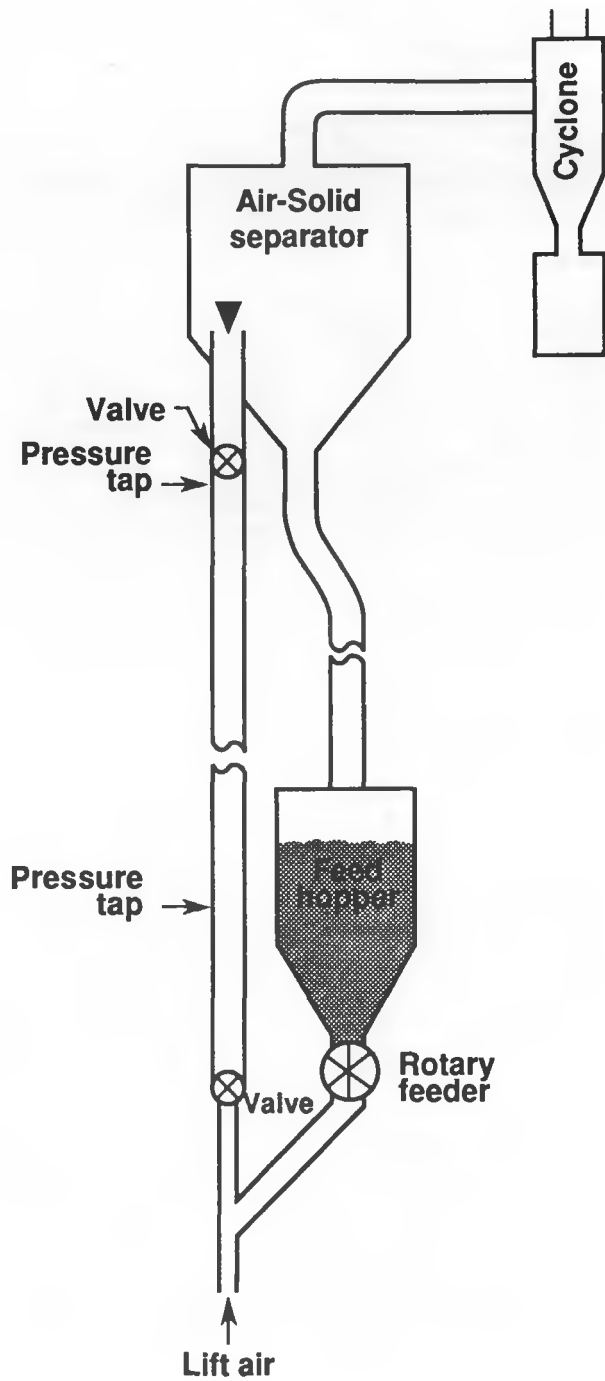


Fig. 3-3. Lift-pipe test apparatus.

Figure 3-4 shows results of a typical trapping experiment. For these data, the air speed of ~ 12 m/s and the solid transport rate of ~ 10 kg/min. are the values that will be used in the pilot plant. By comparing the particle size distributions in the feed material and in the trapped material, one obtains the upward speed of the particles. As shown in the figure, the smallest particles move upward almost as fast as the lifting air. The largest particles move upward at approximately one-half the speed of the air.

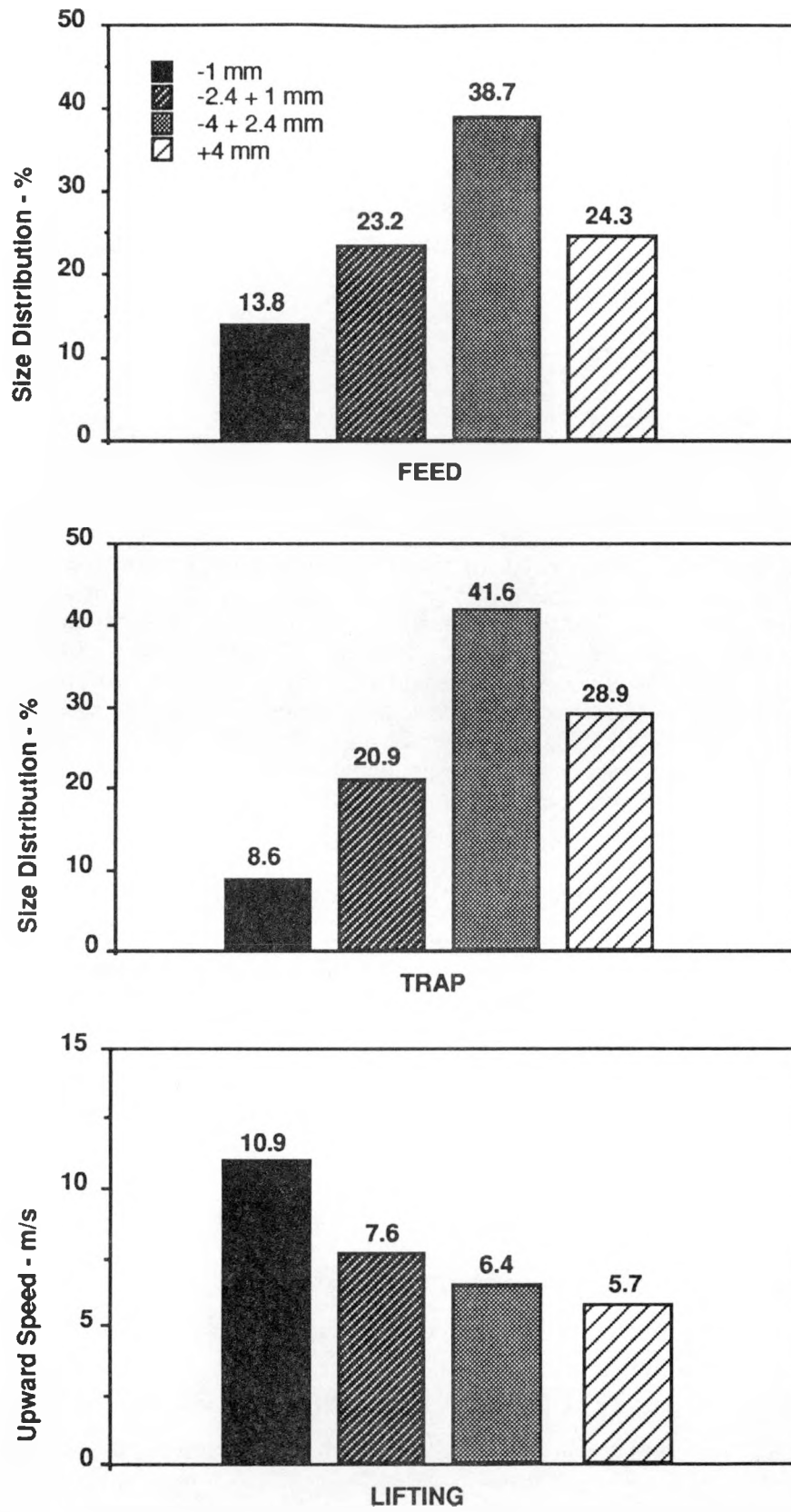


Fig. 3-4. Typical lift-pipe test results (trapping data).

Figure 3-3 shows the positions of two of the pressure taps that were a part of the test apparatus. These taps had a vertical separation of 6 m. Table 3-1 shows the pressure difference between the taps for several air speeds and solid rates. As expected, the pressure difference increases with increasing solid rate and decreasing air speed.

Table 3-1. Typical lift-pipe test results (pressure data).

Air speed (m/s)	Solid rate (kg/min.)	Pressure Diff. (kPa)
11.7	5.3	0.59
11.7	9.9	0.87
11.7	14.7	1.02
9.7	9.9	1.15

3.2 Delayed-Fall Combustor

The delayed-fall combustor provides long residence time and intimate mixing of solid and air. The amount of combustion is controlled by varying the amount of air passing through the unit. Figure 3-5 shows the test model of this combustion unit. The size, arrangement, and spacing of the parallel horizontal rods in the model are the same as will be used in the pilot plant. As shown in the figure, a pair of blocking doors were provided to trap solid flowing between the rods. Solid flow rate was controlled by the size of the feed hopper outlet. The average speed-of-fall is calculated from the solid flow rate and the amount trapped. Table 3-2 shows results of these tests. With no air flow, the average solid speed is independent of solid flow rate. With upward air flow of 0.28 m/s, the solid speed is reduced by about 7%. Using these data, the pilot plant unit was designed to have a residence time of 5 seconds.

Table 3-2. Delayed-fall combustor test results.

Air speed (m/s)	Solid mass flow (kg/min.)	Av. mass trapped (g)	Mean downward particle speed (m/s)
0	11.7	326	0.55
0	17.3	480	0.55
0.28	17.3	518	0.51

3.3 Fluid-Bed Classifier

The fluidized-bed classifier performs four functions:

1. Rejects excess solid from the circulating loop in such a way that rejected material includes the smallest circulating particles.
2. Functions as a surge tank to smooth irregularities in solid loop flow.
3. Provides char combustion as needed to raise the temperature to that required at the retort inlet.
4. Provides an increase in gas pressure to balance the pressure decrease that occurs in the lift pipe.

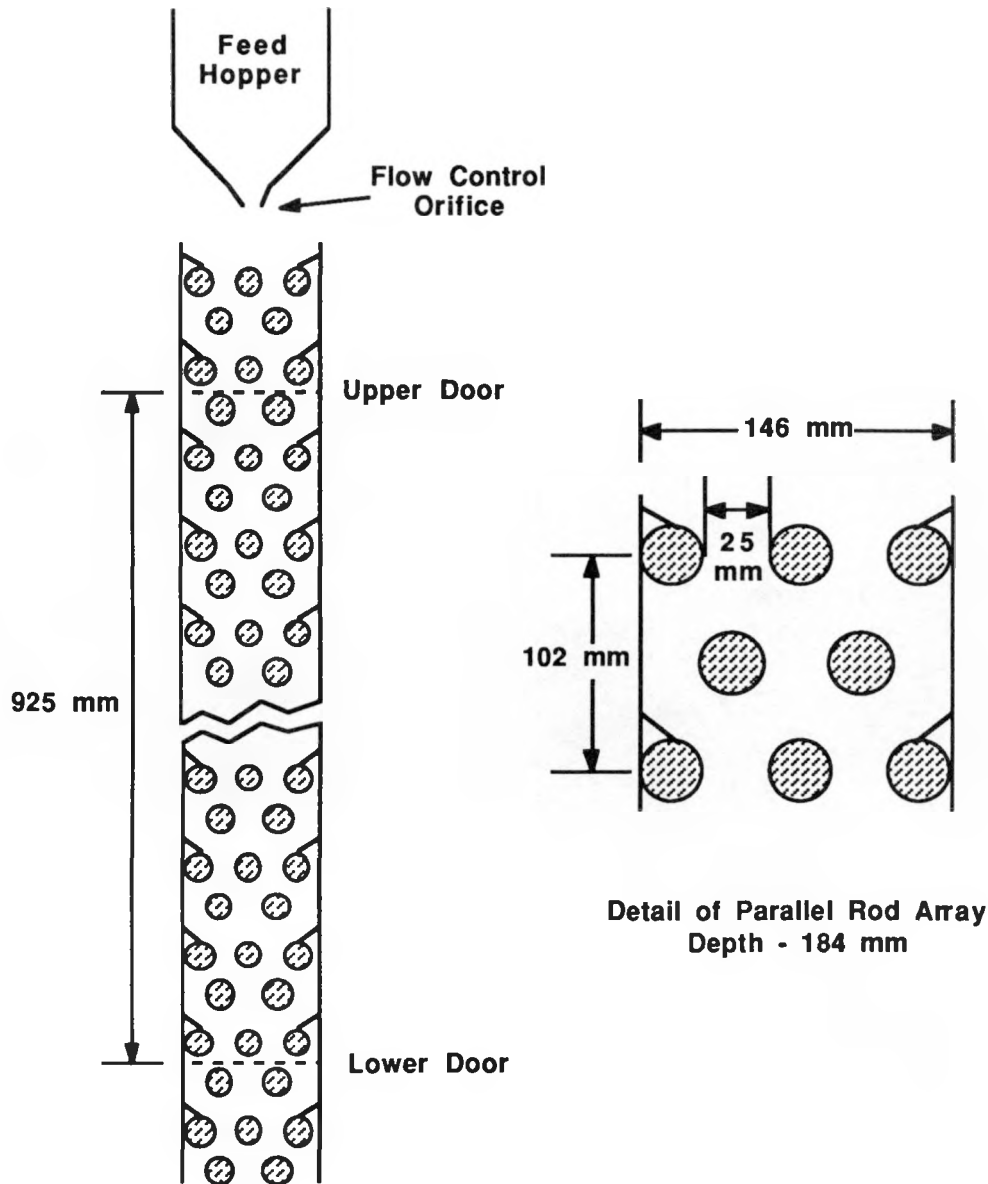


Fig. 3-5. Delayed-fall combustor test model.

Figure 3-6 portrays the test model of the fluidized-bed classifier. In the model, the bed is contained in a 15-cm-diameter tube of lucite. The transparent tube permits observation of particle motion in the bed. Mixed-particle-size shale enters the fluidized bed from the top. The feed rate is controlled by a rotary valve. The shale leaves the bed both at the bottom and at an overflow port on one side. Particle motion in the bed results in size segregation so that the smallest particles concentrate at the top of the bed. Removal from the bottom of the bed is controlled by a rotary valve. In operation, the removal from the bottom is at a lower rate than the rate of feed in at the top; the difference is the rate of side overflow. This overflow contains most of the very small particles. In the hot-recycle retorting system, the material from the bottom of this fluid bed will flow into the pyrolyzer, and material from the side outlet will be rejected. Figure 3-7 is a drawing showing details of the gas distributor plate.

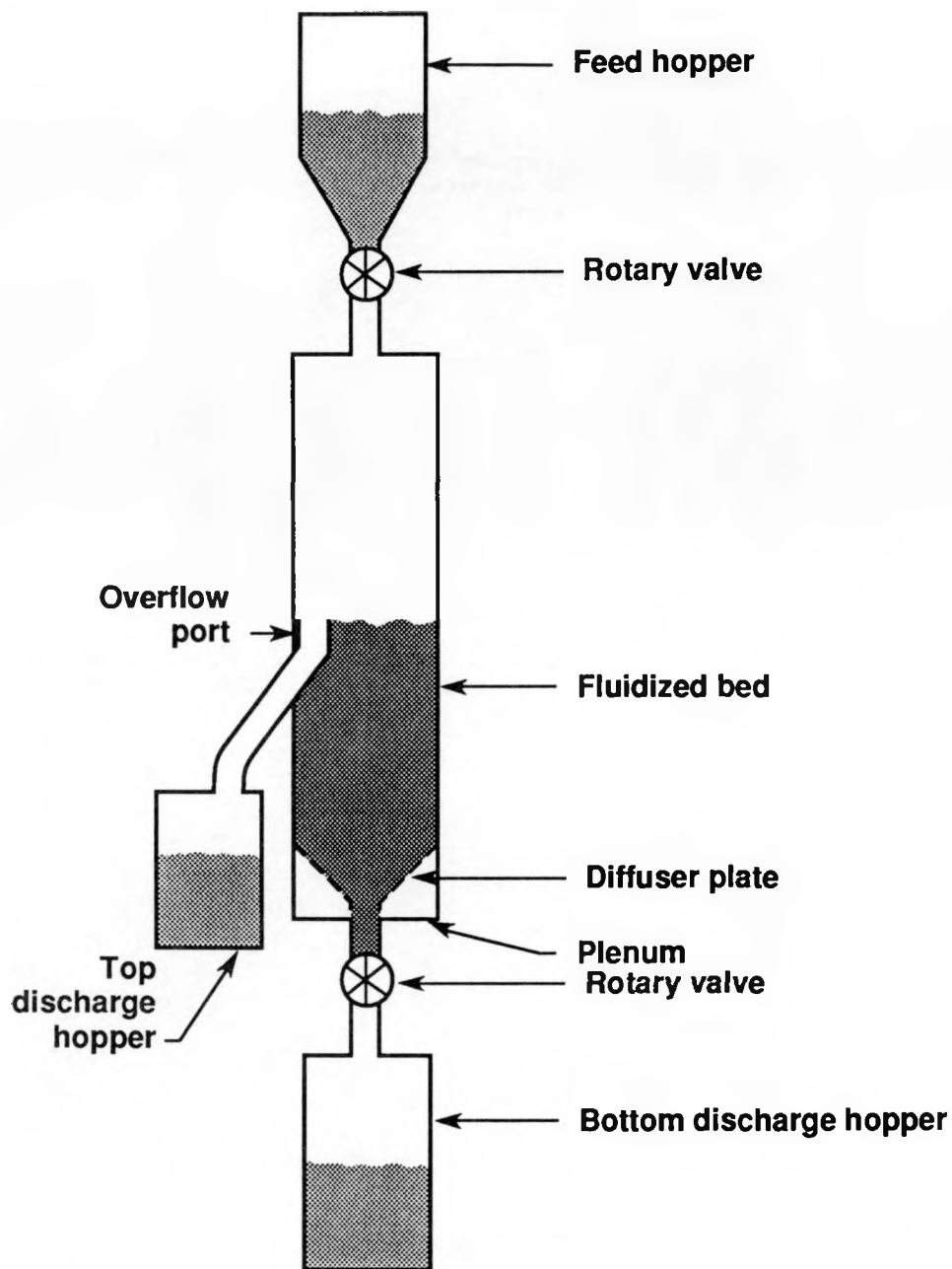


Fig. 3-6. Fluidized-bed classifier model.

Four test conditions were measured. The discharged material was screen analyzed to determine the effectiveness of particle-size segregation. Table 3-3 shows results of these tests. For each test, four particle-size ranges are shown. Also shown are air-flow rates and pressures at various points in the apparatus. The data indicate that the bed will be effective in removing very small particles from the circulating loop. Except for test 4, the observed gas-pressure difference across the bed is approximately that required to balance the pressure drop in the lift pipe.

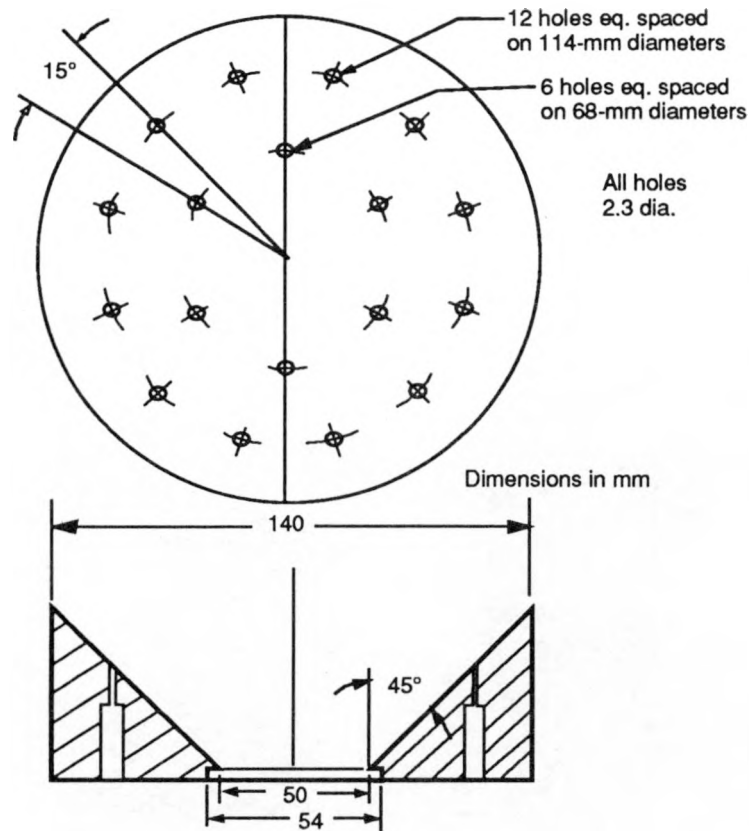


Fig. 3-7. Details of the gas distributor plate.

Table 3-3. Results of particle-size segregation tests.

	Test #1	Test #2	Test #3	Test #4
Air flow vol. (STP L/min.)	861	920	453	287
Plenum pressure (kPa)	81.3	82.7	22.1	10.3
Headspace pressure (kPa)	1.49	1.74	0.50	0.25
Bed pressure diff. (kPa)	3.6	3.4	3.4	2.2
Air-flow speed, lower bed (m/s)	0.97	1.04	0.52	0.33
Air-flow speed, upper bed (m/s)	1.28	1.36	0.68	0.43
Feed rate (kg/min.)	9.11	9.81	9.48	9.42
Ratio of bottom discharge/top discharge	2.86	2.47	2.55	2.44
% in feed				
-7.0 + 2.4 mm	57.3	56.5	57.9	62.9
-2.4 + 1.0 mm	25.0	26.7	24.7	23.8
-1.0 + 0.43 mm	14.2	13.0	13.3	10.7
-0.43 mm	3.5	3.8	4.1	2.6
% in top discharge				
-7.0 + 2.4 mm	36.4	37.0	47.0	65.0
-2.4 + 1.0 mm	26.0	25.2	21.0	21.5
-1.0 + 0.43 mm	26.7	26.0	21.7	10.1
-0.43 mm	10.9	11.8	10.3	3.4
% in bottom discharge				
-7.0 + 2.4 mm	64.6	64.4	62.2	62.0
-2.4 + 1.0 mm	24.6	27.3	26.2	24.8
-1.0 + 0.43 mm	9.9	7.8	10.0	11.0
-0.43 mm	0.9	0.5	1.6	2.3

The fluidized-bed mixer is the unit that mixes the cool, raw shale with the hot, burned shale. Figure 3-8 is a diagram of the test model of this unit. A 15-cm-diameter lucite tube contains the bed. A flat, vertical plate in the center of the tube divides the bed into two stages. The solid material enters the bed at the top of the first stage, moves downward and around the bottom of the plate, and then upward in the second stage to the exit at the top of the second stage. In performing a test in this model, the equipment is brought to steady operation and the solid feed and fluidizing gas are turned off simultaneously. The solid material so trapped is removed and weighed, and its particle size is analyzed. By comparing trapped material with fed material, the residence time as a function of particle size is obtained. Figure 3-9 shows typical results. Residence time varies from 25 seconds for small particles to 45 seconds for large particles. The average residence time in the bed is 35 seconds. The mixing unit in the pilot plant has the same two-stage construction used in the model but has two solid-entry pipes above the top of the first stage. One of these pipes conveys the raw shale; the other conveys the burned shale.

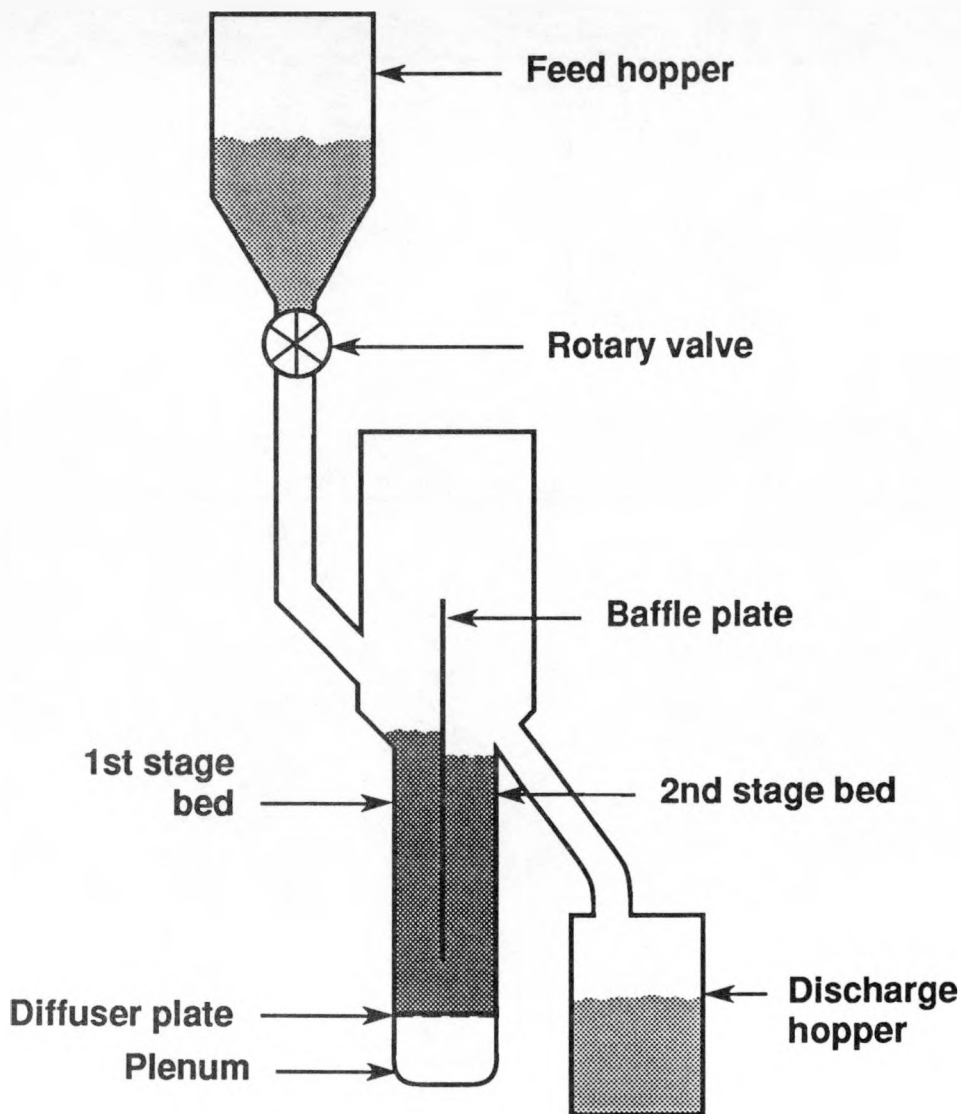


Fig. 3-8. Fluidized-bed mixer model.

The packed-bed pyrolyzer holds the mixed shale for completion of pyrolysis of the raw shale. The pyrolyzer is a plug-flow reaction vessel with radial removal of oil and gas vapor. Figure 3-9 shows construction of the components. Because of previous favorable experience with this type and size of equipment, we did not perform model tests on the pyrolyzer. As the figure shows, a central pipe provides gas to sweep the pyrolysis region thereby reducing loss of oil product by coking and cracking. The residence time of solid in the pyrolyzer can be varied by varying the height of shale in the vessel.

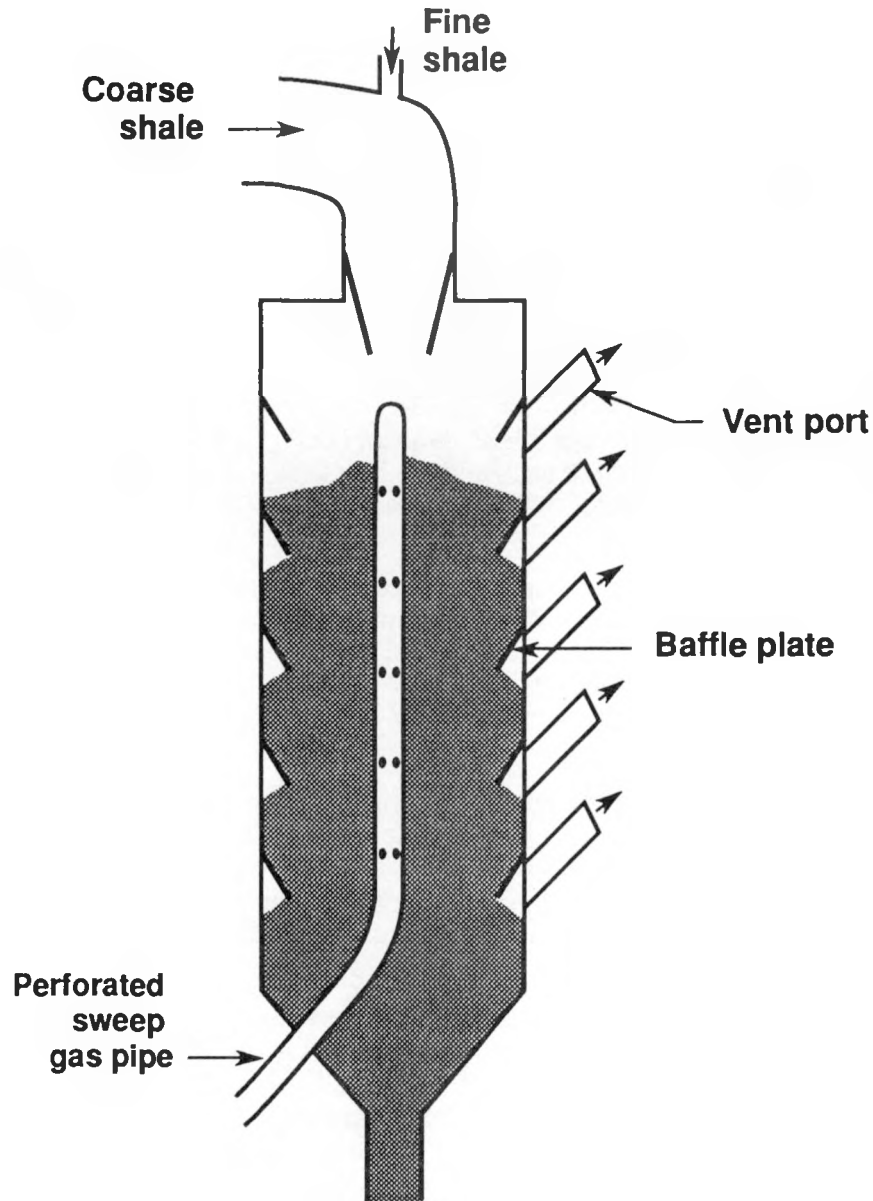


Fig. 3-9. Packed-bed pyrolyzer.

At the end of September, all of the components of the solid-circulation loop had been fabricated and installed in the pilot plant. Work is continuing on ancillary equipment such as gas piping and oil condensers.

4. SHORT-TERM CARBONATE DECOMPOSITION IN GREEN RIVER OIL SHALE

4.1 Abstract

There are no data on the rate of carbonate decomposition in Green River shales for heating times shorter than 10 minutes. The duration of combustion of retorted shale in the HRS process is approximately 1 minute. We have measured the thermal decomposition rate of carbonates during the first minutes of heating at 700 °C. We found that the short-time carbonate-decomposition rate is just about what would be calculated from previous long-term experiments. Approximately 15% of the carbonates in shale will be decomposed in 1 minute at 750 °C, and the decomposition will use the energy produced by burning 5% of the char in retorted shale. The optimum combustion temperature for HRS processes has not been determined. This work suggests that carbonate decomposition is not a factor, at least not up to approximately 750 °C.

4.2 Introduction

Oil shale from the Green River formation of the western United States is made up of a mixture of silicate and carbonate minerals in approximately equal proportions. When this shale is heated, carbonates decompose. Carbonate decomposition requires heat and produces CO₂. The rate of carbonate decomposition increases with temperature.

We are currently producing oil from this shale in an HRS process. In this process, oil is liberated from the shale by the action of heat, and the heat is supplied by the combustion of carbonaceous residue in retorted shale. The heat is conveyed to the raw shale by mixing hot burned shale with cold raw shale.

The hotter the burned shale, the less of it is needed to heat and retort raw shale. However, the rate of carbonate decomposition increases with combustion temperature, and carbonate decomposition takes heat. Thus, a higher combustion temperature requires heat for heating shale and for carbonate decomposition. The net effect can be the combustion of carbonaceous material for carbonate decomposition with little increase in the temperature of the burning shale and with release of much CO₂.

In the HRS process, shale reaches a maximum temperature in the combustor. The total time at combustion temperature in LLNL's HRS system is approximately 1 minute, based on an average of four passes through the combustor. During this time, 15–30% of the CO₂ in the shale has been lost in the experiments to date. The combustion temperatures in these pilot-system experiments have been between 640 and 700 °C. Higher combustion temperatures have not been explored because of materials limits and combustor design.

Laboratory investigations of the rate of carbonate decomposition at constant temperature have been limited to observations of carbonate decomposition in Green River shale at times of 10 minutes and longer over a temperature range of 566–843 °C [4-1]. Campbell [4-2] investigated carbonate decomposition in Green River shale under non-isothermal conditions at heating rates of 2–20 °C/min. Conditions of interest to the HRS process would be rapid heating (5–50 °C/s) followed by isothermal decomposition over time scales of a few seconds to a few minutes and temperatures of 600–800 °C.

This work was initiated to improve our understanding of short-term carbonate decomposition in Green River oil shale. We have measured carbonate-decomposition rates at 700 °C, and compared our results to predictions based on Campbell's work and a recent interpretation of Jukkola's 1953 experimental data by Camp and Braun [4-3].

4.3 Experimental

The experiments consisted of dropping samples of shale into a preheated fluidized bed of sand. The extent of carbonate decomposition was calculated from the CO_2 content of the exit gas.

The material used was Green River shale from the mahogany zone of the Anvil Points mine (AP24C). The sample was retorted according to the Fischer assay procedure (maximum temperature $\sim 500^\circ\text{C}$ for 10–20 min.). The carbonate mineralogy of the Green River shale is complex, but its principal minerals are dolomite ($\text{Ca}(\text{Mg},\text{Fe})(\text{CO}_3)_2$) calcite (CaCO_3). The dolomite crystals tend to be zoned with iron-rich outer surfaces. The sample contained ~ 30 wt% dolomite and 10 wt% calcite. The retorted shale sample contained 24.1 wt% acid-evolved CO_2 .

The retorted shale was ground and sieved to a size range between 20 and 40 mesh. A sample weighing a few grams was dropped into a fluidized sand bed preheated to 700°C . The fluidizing gas was argon flowing at 4.0 liters/minute at room temperature and pressure). The extent of carbonate decomposition was deduced from the concentration of CO_2 and CO in the fluidizing gas. (The CO is assumed to be formed by the reaction of char with CO_2 .) The gas was analyzed every 5 seconds by means of a mass spectrometer.

4.4 Results

Two nearly identical experiments have been carried out. In the first experiment, 2.60 grams of retorted shale were dropped into an 85-g sand bed. The bed temperature fell approximately 10°C (to a minimum of 694°C) with the mixing of the room temperature shale sample into the bed. After the CO_2 concentration returned to zero, a second experiment was made by adding another 2.95 grams of retorted shale; the final bed temperature was about 692°C .

The measured concentrations of CO_2 and CO as a function of time for the two experiments are given in Figs. 4-1 and 4-2. The higher concentration of CO in the second drop is due to the larger

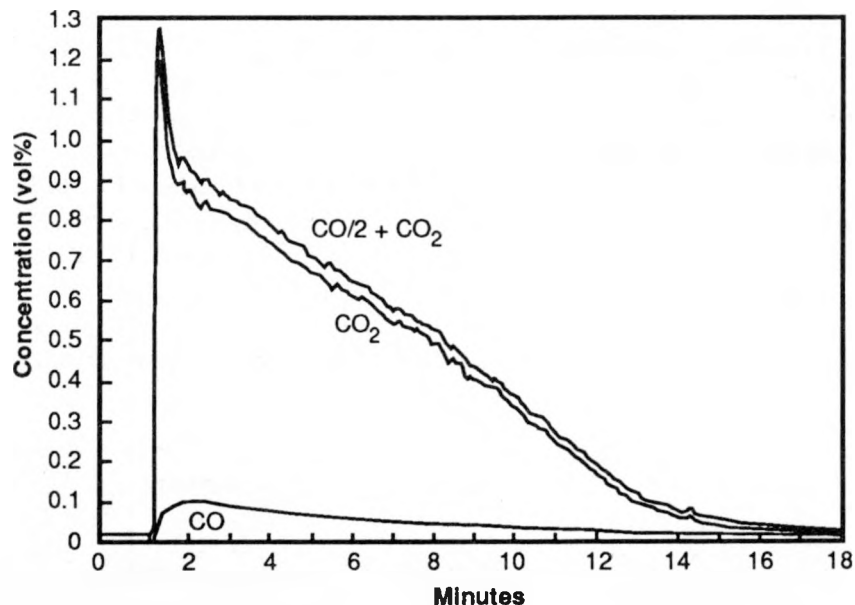


Fig. 4-1. Carbon dioxide evolution from retorted Green River shale heated at 700°C in a laboratory fluidized bed, experiment cd7. Fluidizing gas was argon. The CO_2 concentration is proportional to the rate of carbonate decomposition. Carbon monoxide is assumed to be formed by the char reduction of CO_2 .

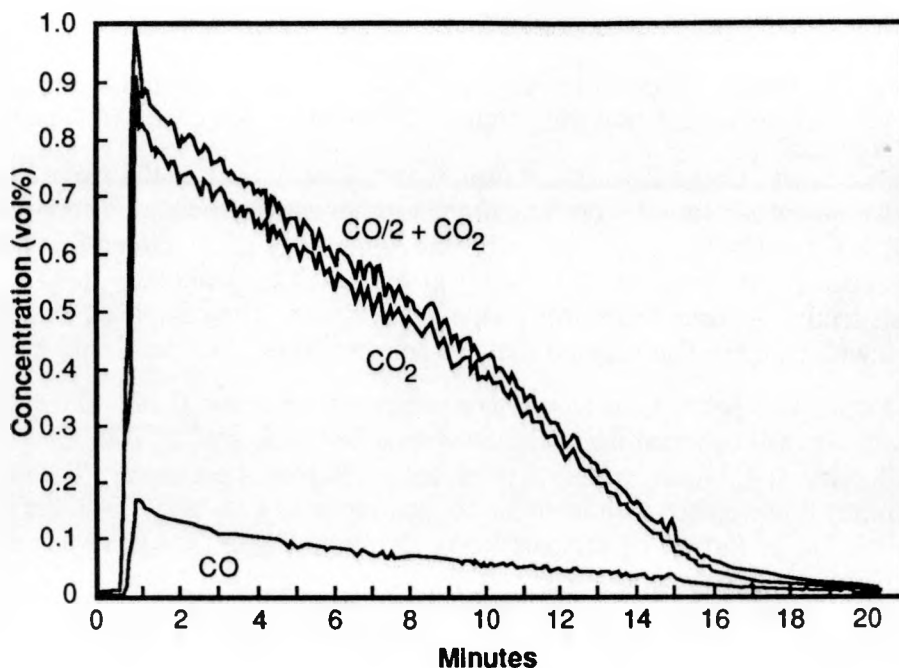


Fig. 4-2. Repeat of the experiment shown in Fig. 4-1 with a slightly larger sample size and faster argon flow rate, experiment cd8.

amount of char in the bed since both samples were in the bed. The concentrations of CO_2 and CO and gas-flow rates were used to determine that 0.521 gram of CO_2 was produced during the first experiment and 0.579 gram of CO_2 was produced during the second experiment. These correspond to releases of 20.0% and 19.6% CO_2 from the first and second samples, respectively.

The CO_2 concentrations we measured from heated shale increased to a peak during the first 15–20 seconds. This peak stands above the trend that follows (see Figs. 4-1 and 4-2) and may be due to combustion of a small fraction of the char by adsorbed oxygen. (We did, however, attempt to eliminate adsorbed oxygen by preheating the shale at 75 °C in flowing argon.) The CO_2 peak may also be due to chemical reactions between carbonates and silicates in Green River shale. The short-time rates of diffusion-controlled solid-state reaction are rapid, and they essentially stop as the reaction-product layer grows. This reaction has been investigated by Kridelbaugh [4-4], who found that the reaction proceeds as kt^n , where n is ~ 0.2 . Kridelbaugh's results suggest that the quartz calcite reaction is 1.5% completed after 20 seconds at 700 °C, and 2.3% completed in the same period of time at 750 °C. This is a much faster initial reaction rate than that predicted by first-order kinetics.

Figure 4-3 shows the fraction of CO_2 released as a function of time for these two experiments; it also shows that, after 1 minute, $12 \pm 2\%$ of the carbonate was decomposed.

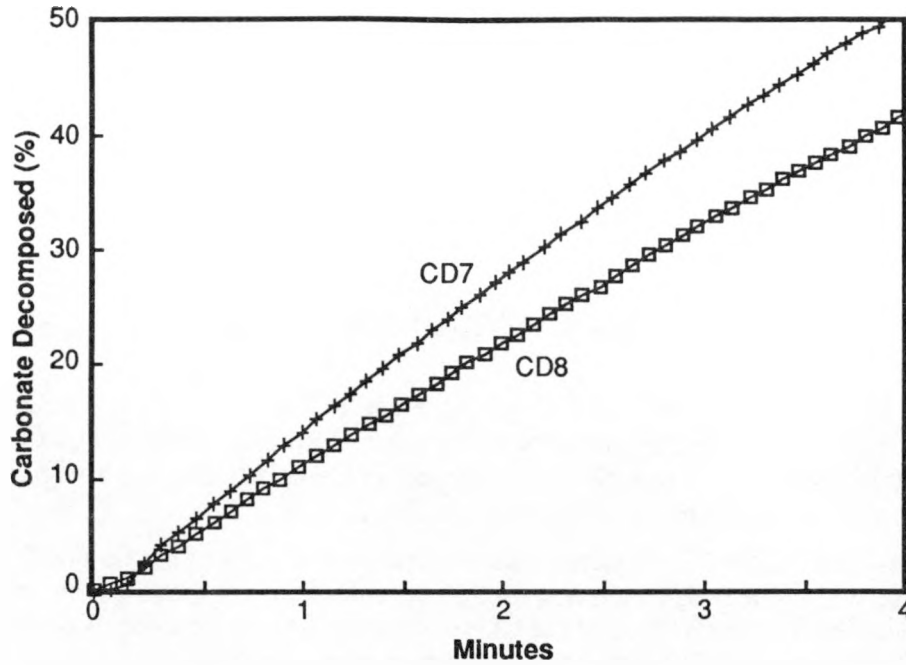


Fig. 4-3. Extent of carbonate decomposition during the first few minutes of heating of Green River oil shale at 700 °C. From integration of the data of Figures 1 and 2.

4.5 Discussion and Conclusions

Figure 4-4 shows a prediction of the extent of carbonate decomposition for this particular shale sample under our experimental conditions based on the work of Camp and Braun. Dolomite is assumed to decompose into calcite and MgO independently of CO₂ pressure (at this temperature).

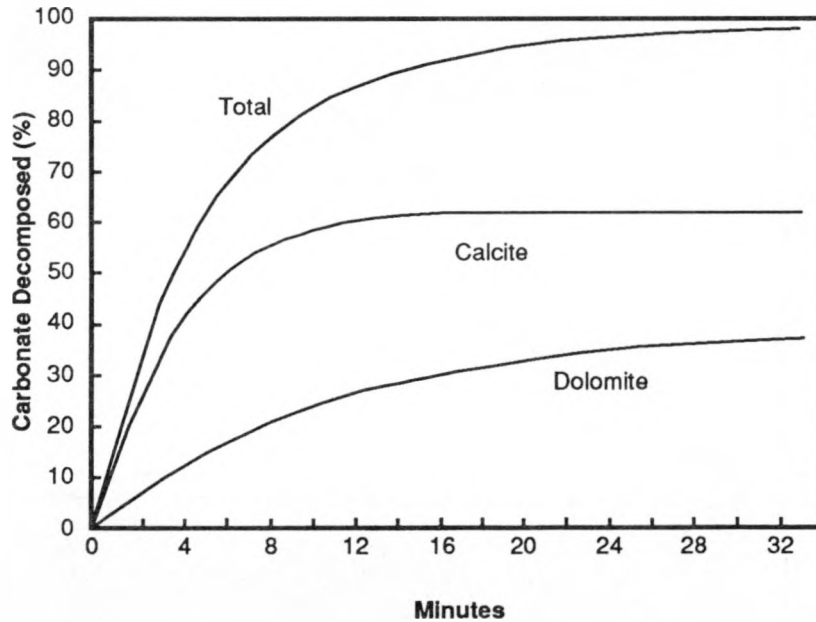


Fig. 4-4. Extent of carbonate decomposition in Green River shale as a function of time at 700 °C calculated from the model of Camp and Braun.

The decomposition reaction was assumed to be first order, and the rate constant was taken to be $4.08 \times 10^7 \exp(-23320/T) \text{ s}^{-1}$. Campbell deduced a rate constant of $1.7 \times 10^{10} \exp(-29089/T) \text{ s}^{-1}$. This constant gives slightly smaller extent of decomposition at temperatures of 700–750 °C than does the Camp and Braun constant, but the differences are less than the differences between our two experiments. We chose to compare to the Camp and Braun model because it was based on isothermal experiments. The decomposition of calcite, both as a component of dolomite and as independent mineral grains, is assumed to be first order, but the rate constant is assumed to depend on CO₂ pressure as follows:

$$1.3 \times 10^{10} \exp(-27680/T) [1 - \text{PCO}_2 / \text{PCO}_{2\text{eq}}] \text{ s}^{-1}$$

where PCO₂ is the actual observed local CO₂ pressure and PCO_{2eq} is the CO₂ pressure below which calcite decomposes at the experimental temperature. Expressed in pascals, PCO_{2eq} is $1.945 \times 10^{13} \exp(-22360/T)$. This model was developed by Campbell and was also part of the model that Camp and Braun fit to the isothermal data of Jukkola.

We have assumed that the CO₂ concentration measured at the exit of the fluidized bed is twice the average value within the bed, which was used in the calculation of the rate constant. The rate constant was calculated for each value of the CO₂ concentration, that is, every 5 seconds of the experiment. (The intraparticle CO₂ pressure is higher, perhaps 1 atm.)

A comparison of our experimental values of carbonate decomposition to the calculated values is given in Fig. 4-5. At one minute, the calculated value (at 700 °C) is about 16% carbonate decomposition compared to experimental values of 11 and 13%. The calculated value for 1 minute at 680 °C is 10%. These results suggest that the model of Camp and Braun can be used to predict short-term carbonate decomposition.

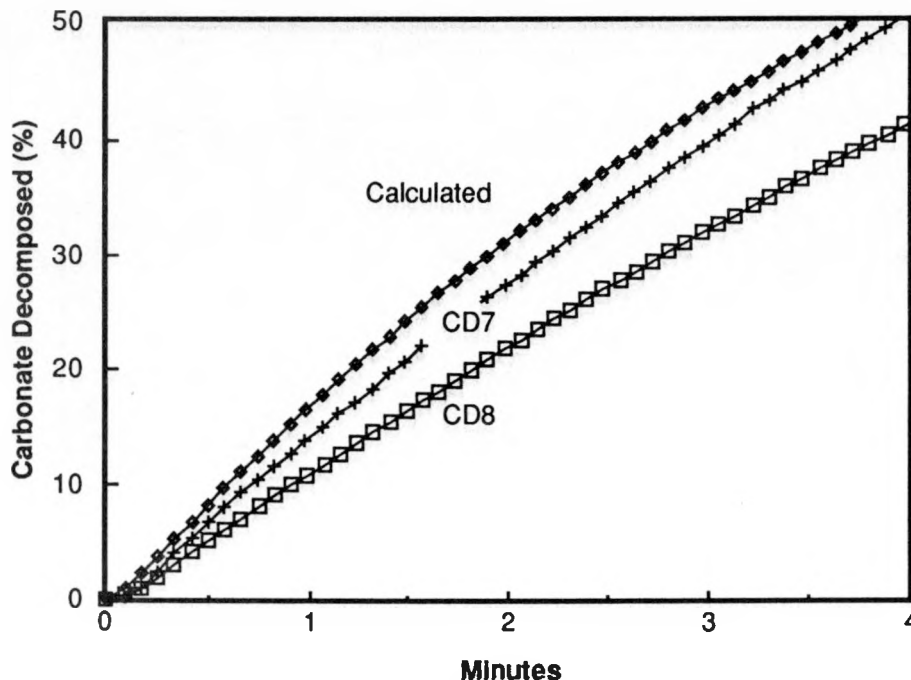


Fig. 4-5. Comparison of experimental values of short-term carbonate decomposition to calculated values.

Under the CO_2 pressure expected in a real combustor (nearly 10%), no thermal decomposition of calcite is allowed at temperatures below 770°C except for reactions with silicates. At 750°C for example, the extent of carbonate decomposition from dolomite alone is calculated to be 14% in 1 minute, as shown in Fig. 4-6.

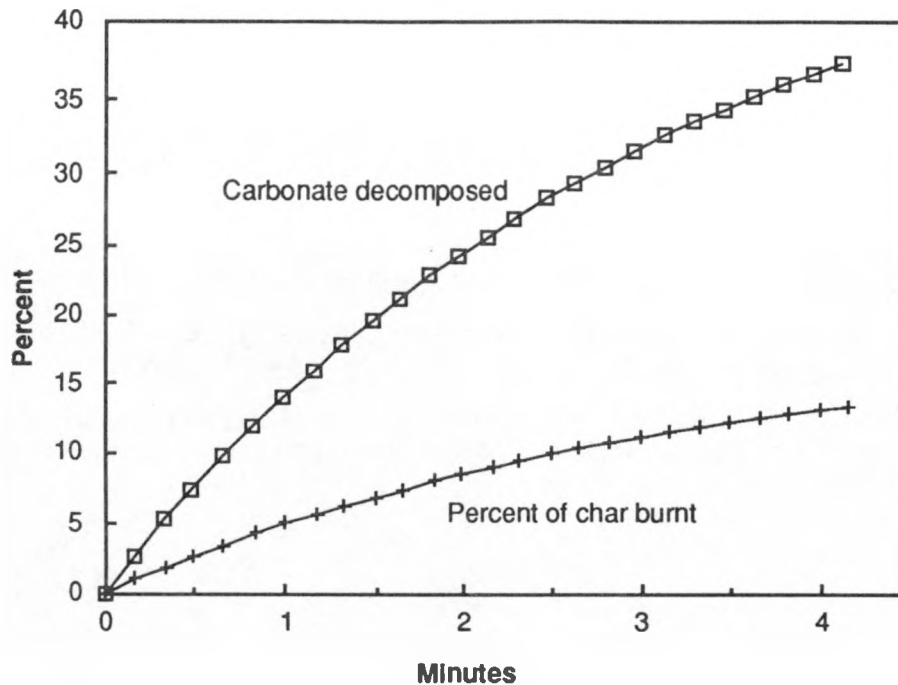


Fig. 4-6. Percent thermal carbonate decomposition at 750°C calculated from the Camp and Braun model, showing the fraction of char required. Based on a retorted shale containing 45% carbonates, mostly dolomite, and 2.5 wt% char.

The difference between the 20% CO_2 release observed and the 23% expected, based on acid-evolved CO_2 , may be due to attrition and loss of some of the retorted shale sample out of the fluidized bed. Taylor and Beavers [4-5] report a rate of attrition for retorted shale of 3–5% per minute for the first 10 minutes of fluidization. This may also explain why the final 20% of carbonate decomposition is faster for the experiments than predicted by the Camp and Braun model. In any case, attrition does not affect the short-time results very much, and they are of principal interest in this report.

Why is the extent of carbonate decomposition in shale processed in our recycle pilot retorts higher than measured in our experiments and higher than predicted by models based on other experiments? Carbonate decomposition is accelerated by the action of steam, according to Campbell. Also, carbonates may be decomposed by chemical reaction as well as by the action of heat. During shale combustion, iron sulfides burn and release SO_2 . This SO_2 reacts with carbonates, displacing CO_2 . A shale containing 1 wt% sulfur will show a 5% carbonate decomposition due to this displacement reaction. Carbon dioxide release by this displacement reaction does not require heat; in fact, the reaction is strongly exothermic.

We conclude that the Camp and Braun model or the Campbell rate expressions can be used to extrapolate short-time carbonate decomposition for Green River shale over the temperature range up to at least 750°C .

The present experiments and model suggest that approximately 15% of the carbonate in Green River shale will be *thermally* decomposed in 1 minute at 750 °C during combustion and that ~5% of the char in retorted shale of average grade will be required for such decomposition.

4.6 References

- 4-1. E. E. Jukkola, A. J. Denilauer, H. B. Jensen, W. I. Barnet, and W. I. R. Murphy, "Thermal Decomposition Rates of Carbonates in Green River Oil Shale," *Ind. Eng. Chem.* **45**, 2711 (1953).
- 4-2. J. H. Campbell, *The Kinetics of Decomposition of Colorado Oil Shale: II. Carbonate Minerals*, Lawrence Livermore National Laboratory, Livermore, Calif., UCRL-52089 Part 2 (1978).
- 4-3. D. W. Camp and R. L. Braun, *Carbonate Decomposition Reaction Scheme and Kinetics*, Lawrence Livermore National Laboratory, Livermore, Calif., UCID-16986-86-3 (1986).
- 4-4. S. J. Kridelbaugh, "The Kinetics of the Reaction: Calcite + Quartz = Wollastonite + CO₂ at Elevated Temperatures and Pressures," *Amer. J. Sci.* **273**, 757 (1973).
- 4-5. R. W. Taylor and P. L. Beavers, "Oil Shale Loss from a Laboratory Fluidized Bed," in *Proceedings of the 22nd Oil Shale Symposium* (Colorado School of Mines Press, Golden, 1989), p. 138.